**RAA 2021** Vol. **21** No. **4**, 106(10pp) doi: 10.1088/1674-4527/21/4/106

*http://www.raa-journal.org* *http://iopscience.iop.org/raa*

*Research in Astronomy and Astrophysics*

# Signature of the 27-day variation in hemispheric sunspot activity and asymmetry during 2010–2015

Prithvi Raj Singh[1], Ahmad Islam Saad Farid[2], Tarun Kumar Pant[3] and Abhay Kumar Singh[1]

[1] Department of Physics, Banaras Hindu University, Varanasi-221005, India; *prithvisingh77@gmail.com*
[2] Physics and Chemistry Department, Faculty of Education, Alexandria University, Alexandria-21526, Egypt; *saadfarid@alexu.edu.eg*
[3] Space Physics Laboratory, VSSC, Thiruvananthapuram-695022, India

Received 2020 August 18; accepted 2020 November 2

**Abstract** In the present work, we study the time evolution, significance of the N-S asymmetry excesses presented as a function of the solar cycle and prominent rotational periods (∼27 d) separately for the northern and southern hemispheres. We have investigated short-term variations of the hemispheric solar activity (sunspot numbers and sunspot areas) during the time period 2010–2015, which covers the ascending and the maximum phase of solar cycle 24. We have implemented the Lomb-Scargle periodogram and continuous wavelet transform power spectrum techniques to study the time evolution and dominant rotational periods separately for the northern and southern hemispheres, and whole solar disk. Our results showed that the northern hemisphere exhibited longer solar synodic periods than the southern hemisphere, indicating that the northern hemisphere has a lower rotation rate. Moreover, the northern hemisphere was found to be dominant before transferring to the southern hemisphere during mid-2013. Also, the sunspot areas clearly demonstrated a two-peak structure of solar activity in the northern and southern hemispheres respectively during 2012 and 2014. The statistical significance of the southern hemisphere affirmed enhanced excess during the maximum phase of solar cycle 24.

**Key words:** Sunspots — Sunspot Area — Asymmetry — Solar Cycle

## 1 INTRODUCTION

Numbers of sunspots observed on the solar disk are the longest observational solar data set used to explore solar activity and its temporal variations. Such variability is represented by various indices such as sunspot numbers (SSNs), the 10.7 cm solar radio flux, sunspot areas (SSAs), X-ray emission from the solar corona, solar flare indices, etc. All these indices show periodic variations over days to years (Chowdhury et al. 2013; Hathaway 2015; Kilcik et al. 2018; Singh et al. 2019a,b and references therein). The most significant periods are 11-year solar cycle variation and Bartels rotation (Bartels 1934) of 27 d. The significant periodicity (27-day) of solar activity represents the solar rotational period, which is related to the dynamo effect on the Sun. The periodic behaviors associated with the hemispheric data of solar activity (SSN and SSA) are manifestations of processes governing the solar rotational phenomena. The 27-day solar rotational period and its subharmonics are also detected in galactic cosmic ray and geomagnetic index time series with high amplitude (Poblet & Azpilicueta 2018; Chowdhury & Kudela 2018; El-Borie et al. 2019). This ∼27 d period is known to be related primarily to large-scale solar magnetic fields (Balthasar & Schüssler 1984).

Gradually, however, it became evident that the northern and southern solar hemispheres are not identical as they do not exhibit similar behavior all the time. These hemispheric differences are usually known as the north-south (N-S) asymmetry. Several manifestations of solar activity were previously investigated to study the N-S asymmetries revealing that they are a fundamental characteristic of solar activity. Various solar activity indices such as SSN, solar flares, filaments, prominences, radio and gamma-ray bursts, coronal emission, solar magnetic fields and others are utilized to analyze the asymmetry phenomena (Waldmeier 1971; Howard 1974; Rusin 1980; Swinson et al. 1986a; Carbonell et al. 1993; Knaack et al. 2004; Gigolashvili et al. 2005; Oliver & Ballester 1994; Ataç & Özgüç 1996; Li et al. 2009, 2010;

Temmer et al. 2006; Chowdhury et al. 2013; Javaraiah 2016, 2019; Leussu et al. 2017; Chowdhury et al. 2019; Singh et al. 2019a).

White & Trotter (1977) observed asymmetry in the solar magnetic field cycle in the SSA in the northern and southern hemispheres of the Sun. Vizoso & Ballester (1990) reported some common features in the behavior of N-S asymmetry in various forms of solar activity such as sunspots, flares and SSA. Carbonell et al. (1993) examined N-S asymmetry and found it was statistically highly significant in SSN and SSA. The hemispheric asymmetry of the solar activity phenomenon is considered as an essential aspect of the solar dynamo action, which in turn is a subject matter for research as it holds the key to understanding the very origin of the solar cycle and activity. Several models to understand the solar dynamo have been developed (Antonucci et al. 1990; Pulkkinen et al. 1999; Temmer et al. 2002; Charbonneau 2020). Chowdhury et al. (2013) investigated the solar dynamo process using a non-linear dynamo model in view of N-S asymmetry observed in different solar indices.

The objective of the present work is to study temporal variation in sunspot activity of the Sun on the time scale of the solar rotation period. Daily data on SSNs and SSAs during the ascending phase (including maximum phase) of solar cycle 24 (2010–2015) for northern, southern and the full solar disk have been examined. Spectral and statistical analysis is employed for this investigation.

## 2 METHODS AND DATA ANALYSIS:

In the present study, we rely on the time series data of daily SSNs and SSAs separately for the northern, southern and the whole solar disk, from 2010 January 1 to 2015 December 31 that include ascending and maximum phases of solar cycle 24. The time series of SSN is provided by `http://sidc.oma.be/silso/newdataset` while data on the SSA are downloaded from `https://solarscience.msfc.nasa.gov/greenwch/daily_area.txt`.

The daily SSN and SSA for northern, southern and the entire solar disk separately are used to investigate the asymmetry and periodicities present therein. The periods are inferred through Lomb-Scargle periodogram (LSP) and the continuous wavelet transformation analysis method. Also, periodic variations in the N-S asymmetry of the SSNs and SSAs are examined. Periodic variations of solar activity evolve in a complex wave-like function which exhibits asymmetry in both hemispheres. In this study, periodicities around and below the ∼27-day period are defined as short-term periodicities, and only those detected periods that are above the 95% confidence level are taken into account.

As has been found, the asymmetry based on absolute asymmetry (N-S) is enhanced near the cycle maximum (Temmer et al. 2006) and solar activity would dominate typically in the hemisphere where the maximum sunspot group number is the largest (Li et al. 2002), so in this study we consider the daily value of SSN and SSA of N-S hemispheres for calculating absolute asymmetry for each year during the maximum phase of solar cycle 24. The absolute asymmetry index (A), chosen to prevent the presence of spurious periods in the spectrum (Ballester et al. 2005), is determined as

$$\mathrm{Absolute\ Asymmetry(A)} = \mathrm{N} - \mathrm{S}\,, \tag{1}$$

where N and S represent either the SSN or the SSA, as the case may be, in the northern and southern hemispheres of the Sun respectively. If absolute asymmetry A>0, the northern hemisphere dominates, and if A<0, the southern hemisphere dominates. In this study, we used the periodic behavior of absolute asymmetry instead of the normalized asymmetry. Ballester et al. (2005) gives a fact that the periodicities obtained by normalized asymmetry are misleading as well as changing the general shape of the power spectrum due to the presence of (N+S) in the denominator.

Here, we apply paired Student's t-test and the significance of the asymmetry. The test statistic $t$ is defined as

$$t = \frac{\overline{D}}{S_{\overline{D}}} = \frac{\frac{(\sum D_i)}{n}}{\sqrt{[\frac{\sum D_i^2 - (\sum D_i)^2/n}{n(n-1)}]}}\,, \tag{2}$$

where $D_i$ is the difference between the northern and southern hemisphere SSA and SSN, $\overline{D}$ is the mean of $n$ differences, $S_{\overline{D}}$ is the standard deviation for $n-1$ degrees of freedom, and $n$ is the number of pairs in the northern and southern hemispheres of the Sun. We consider preselected error probability $(\alpha) = 0.05$, i.e., the difference between northern and southern hemispheres of SSA and SSN is statistically significant at a 95% level (Temmer et al. 2002, 2006; Chowdhury et al. 2013). We used a 95% significance monthly value which is plotted for the northern and southern hemispheres (Fig. 9(a) and 9(b)).

### 2.1 Lomb-Scargle Periodogram:

We have applied the LSP technique which is an appropriate algorithm for the analysis of unequally spaced data. The LSP is an important time-frequency analysis method which is obtainable from a statistical analysis of a time series (Lomb 1976; Scargle 1982). This periodogram technique is useful for assessing the statistical confidence by computing the false alarm probability (FAP). For a time series $X_i = X(t_i)$, $i = 1, 2, ..N$, this periodogram can be defined as a function of frequency $\omega$ as (Lomb 1976; Scargle 1982)

$$P_N(\omega) = \left(\frac{1}{2\sigma^2}\right) \cdot \left\{ \frac{\left[\sum_{i=1}^{N}(X_i - \overline{X})\cos\omega(t_i - \tau)\right]^2}{\sum_{i=1}^{N}\cos^2\omega(t_i - \tau)} + \frac{\left[\sum_{i=1}^{N}(X_i - \overline{X})\sin\omega(t_i - \tau)\right]^2}{\sum_{i=1}^{N}\sin^2\omega(t_i - \tau)} \right\}, \tag{3}$$

where $\overline{X} = \frac{1}{N}\sum_{i=1}^{N}(X_i)$ and $\sigma^2 = \frac{1}{N-1}\sum_{i=1}^{N}(X_i - \overline{X})^2$ are respectively the mean and total variance of the time series and the time shift interval $\tau$ is defined by the relation

$$\tan(2\omega\tau) = \frac{\sum_{i=1}^{N}\sin 2\omega t_i}{\sum_{i=1}^{N}\cos 2\omega t_i}. \tag{4}$$

### 2.2 Continuous Wavelet Transformation:

The temporal evolution of the detected periods is estimated by using the continuous wavelet transform technique. The continuous complex Morlet wavelet transformation function is employed with $\omega_o = 6$. In this technique, the thin black contours within a cone of influence signify periods above the 95% confidence level (Torrence & Compo 1998)

$$\psi_o(\eta) = \pi^{-1/4}e^{i\omega_o\eta}e^{-\eta^2/2}, \tag{5}$$

where $\omega_o$ is a non-dimensional frequency and $\eta$ is the Fourier time period.

## 3 RESULTS

Presented in Figures 1 to 8 are the short-term variations around the solar rotational cycle (27-day) of SSNs and SSAs for northern, southern and the whole solar disk, and their absolute asymmetry. It is easily seen that each figure comprises four panels. The upper panel (a) displays the time profile of the daily time series (in red) under investigation for the time span 2010–2015. As the daily data are highly fluctuating, the 30-day moving average data are also plotted (in black) in the same panel to highlight the trend and the general behavior of the data. It enables us to easily associate the data with the phase of solar activity. The 30-d moving average displays a double-peak structure during the ascending phase of solar cycle 24. In the middle row, the wavelet power spectrum (WPS) and the global wavelet spectrum (GWS) are shown in panels (b) and (c), respectively. The lowermost panel in each figure represents the normalized LSP. Both spectral methods are only displayed in the period range of 16–36 d, as the present study is concerned primarily with period at ~27 d. So, the subharmonics (not depicted here) of this period are out the concern of the present work. The red-dashed lines in panels (c) and (d) indicate the 95% significance level estimated respectively by the red noise and the FAP.

The detected periodicities that are above the 95% confidence level are taken into account and inserted in each figure by both methods, i.e., WPS and LSP. In WPS, periodicities with a 95% confidence level are the dark region areas surrounded by solid curves. The GWS is the wavelet power at each period-scale averaged over time and similar to the Fourier spectra. Both spectral methods reveal periods close to the synodic period as described below.

Figures 1 and 2 represent the SSN and SSA respectively for the northern hemisphere. In Figure 1(b), we observed contours for periods between 16–32 d extending first from Feb 2011–October 2011 and then from April 2012–May 2013. However, periods between 25–30 d are sporadically found between September 2013 and late 2016. The corresponding GWS of SSN manifests a prominent peak at 26.6 d (Fig. 1(c)). In Figure 2(b), periods between 16–36 d persist from Feb 2011–March 2012, and periods between 16–32 d during Jan–April 2013. However, periods between 20–30 d prevail during Oct 2013–Jan 2014, between 19-35 d during May–June 2014, and between 16–34 d during April-July 2015. The corresponding GWS of SSA shows the dominant period at 26 d (Fig. 2(c)). Both Figures 1(d) and 2(d) indicate a significant period at 28.2 d for SSNs and SSAs for the northern hemisphere as indicated by LSP method.

Similarly, Figures 3 and 4 depict, in turn, the SSN and SSA for the southern hemisphere. In Figure 3(b), periods between 22–34 d are prominent during April–July 2012, while those between 16–35 d during June–Dec 2014. The corresponding GWS features the dominant period at 26.5 d (Fig. 3(c)). In Figure 4(b), periods between 16–34 d are prominent during July 2012 and Dec 2013–Jan 2014. Also, periods between 16–36 d are observed during May 2014–Dec 2014. The corresponding GWS shows the dominant period at 27 d (Fig. 4(c)). The LSP method (Figs. 3(d) and 4(d)) detected the significant periods at 27.2 and 27.1 d for SSN and SSA, respectively.

Likewise, Figures 5 and 6 display the SSN and SSA for the full solar disk. The activity of the whole disk (SSN and SSA) provided different information than that for the northern or southern hemispheres. In Figure 5(b), we see a period contour between 18–33 d becoming prominent during 2012. Similarly, periods between 20–35 d attain significance during April–Nov 2014, whereas another group of periods dominate between 22–34 d during May–July 2015. The corresponding GWS shows the dominant period at 26 d (Fig. 5(c)). In Figure 6(b), periods between 22–32 d are significant during June 2012 and those between 16–32 d during Dec 2013–Jan 2014.

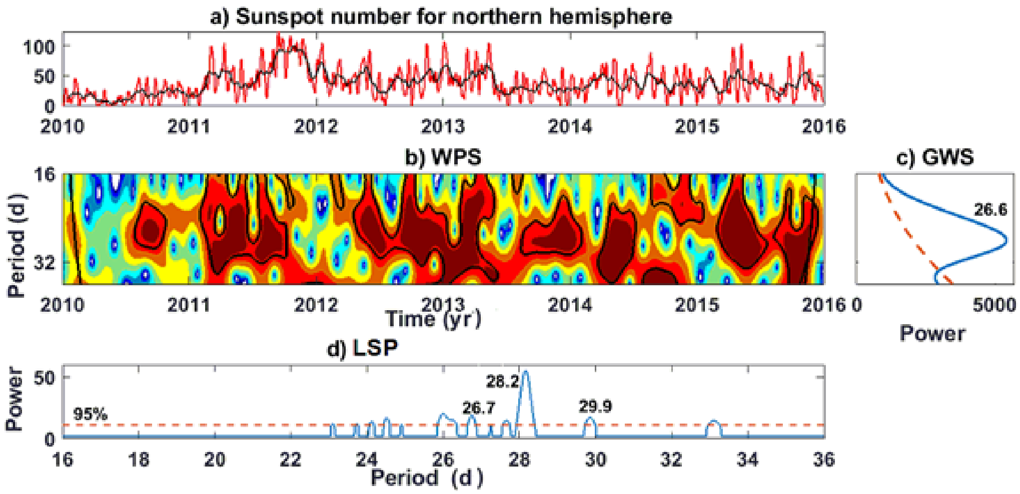


**Fig. 1** (a) Daily time profile (in *red*) and 30-day moving average data (in *black*), (b) WPS, (c) GWS and (d) LSP for daily SSN (northern hemisphere) during 2010–2015.

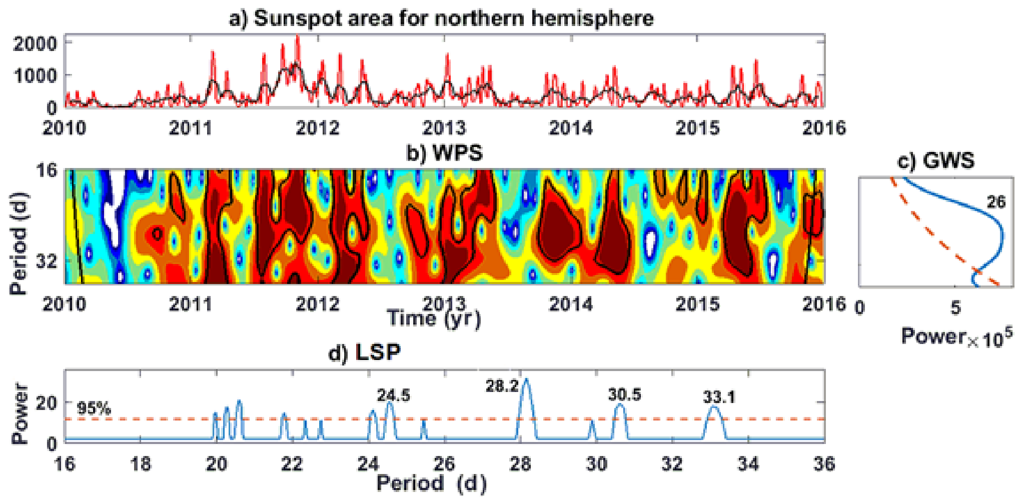


**Fig. 2** (a) Daily time profile (in *red*) and 30-day moving average data (in *black*), (b) WPS, (c) GWS and (d) LSP for daily SSA (northern hemisphere) during 2010–2015.

Periods between 16–32 d are found during Dec 2013 - Jan 2014 and April-July 2014 as well as between 16–36 d during Sept-Dec 2014. The corresponding GWS features the dominant period at 26.6 d (Fig. 6(c)). Figures 5(d) and 6(d) reveal close significant periods at 26.1 d and 26.2 d for SSN and SSA, respectively by the LSP method.

The spectral analysis of the absolute asymmetry for SSN and SSA is depicted in Figures 7 and 8 respectively. The absolute asymmetry as estimated by Equation (1) displays the daily variation of SSNs and SSA in the time interval 2010–2015 in Figures 7(a) and 8(a). The variation of the northern hemisphere is dominant up to 2012, while the southern hemisphere during 2013–2015. Also, the periodic variations of the absolute N-S asymmetry of the SSNs and SSAs are studied. Several contours between 16–35 d are dominant during the years 2011, 2012, 2013 and 2014 (Fig. 7(b)). The corresponding GWS shows significant periods at 27.6 d (Fig. 7(c)). In Figure 8(b), periods between 16–33 d are significant during mid–2012 and between 16–32 d during Nov 2013–Jan 2014. Two periods between 16–32 d are observed during April–June 2014 and those during 16–36 d during August to Dec 2014. The corresponding GWS features the dominant period at 29.4 d (Fig. 8(c)). The LSP method of absolute asymmetry for SSN and SSA exhibits periodicity at 26.1 d and 26.2 d, respectively (Figs. 7(d) and 8(d)).

In Figure 9(a) and 9(b), the cumulative values before the transition phase from the northern to southern hemisphere show maximum spacing present in both solar activity parameters SSN and SSA. The cumulative analysis of SSN and SSA during the maximum phase of solar cycle 24 confirms northern hemisphere dominance at

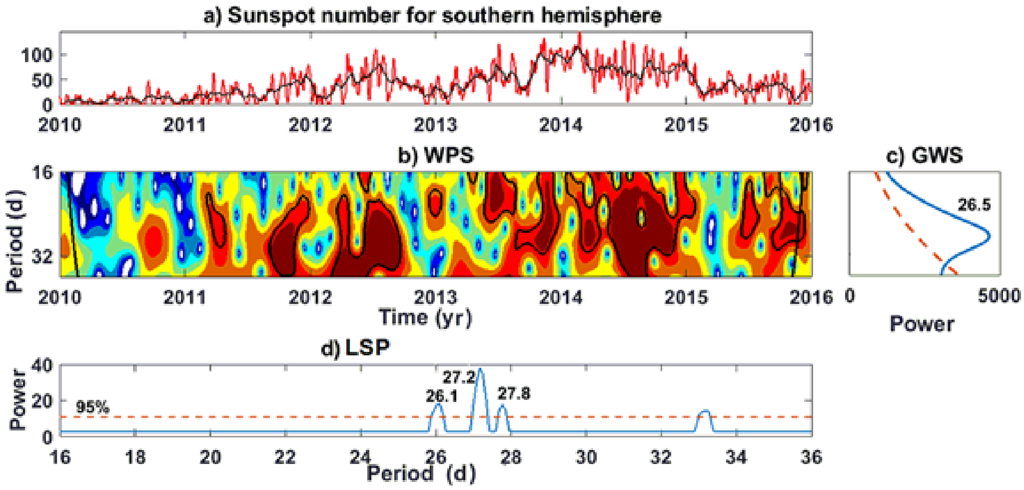


**Fig. 3** (a) Daily time profile (in *red*) and 30-day moving average data (in *black*), (b) WPS, (c) GWS and (d) LSP for daily SSN (southern hemisphere) during 2010–2015.

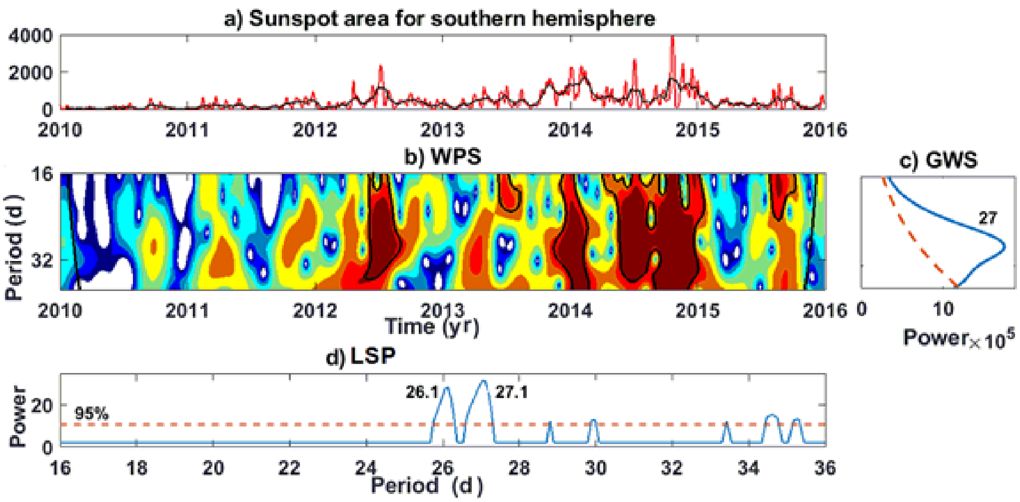


**Fig. 4** (a) Daily time profile (in *red*) and 30-day moving average data (in *black*), (b) WPS, (c) GWS and (d) LSP for daily SSA (southern hemisphere) during 2010–2015.

the rising phase of the cycle, after transition phase for southern hemispheric dominance. The cumulative analysis of northern and southern hemispheres for SSN and SSA affirms that the transition phase occurs in mid-2013 which is clearly visible in Figure 9(a) and 9(b). Thus, the Gnevyshev gap provides physical information about the solar activity being a superposition of the northern and southern hemispheres.

The paired Student's t-test is applied to determine the significance of the difference between the northern and southern hemispheres of SSNs and SSAs. In Tables 1 and 2, the result of the Student's t-test is given as the percentages of significant months concerning the total number of months during the period 2010–2015. In the present study, about 50% of all months reveal a highly significant N-S asymmetry for SSN as well as for SSA which is 66%. The percentage of months with significant activity of northern and southern hemispheres in SSN and SSA is similar for the periods 2011 and 2014. The southern hemisphere covers almost thrice as much significant months than the northern in the period 2013, (see Tables 1 and 2). According to this result, solar activity during the period 2010–2015 is non-symmetric for the northern and southern hemispheres. .

## 4 DISCUSSION AND CONCLUSION:

The results of the present study indicate that different features of periods are seen when the activities of the northern and southern hemispheres are considered separately (SSNs and SSAs), and also across the whole solar disk as one. Figures 1–8 clarify that the southern and northern hemispheres do not exhibit similar rotational

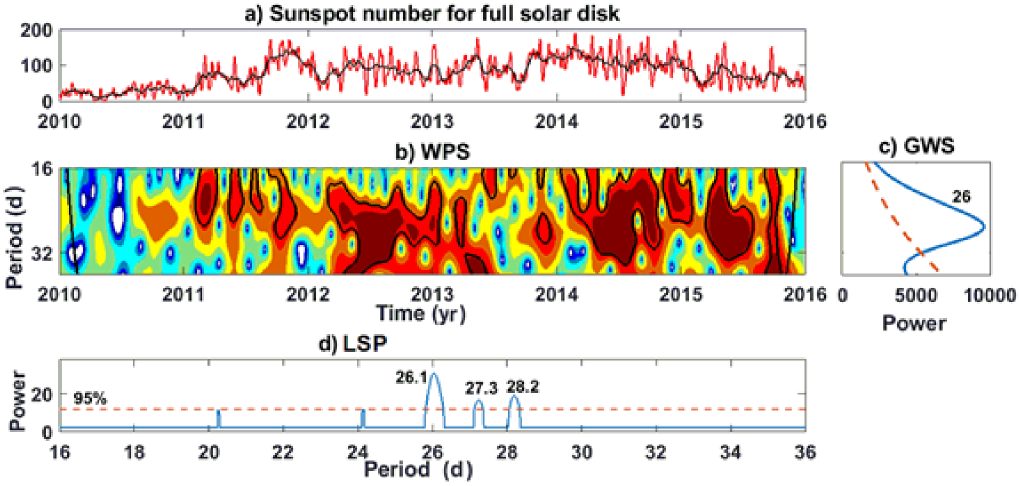


**Fig. 5** (a) Daily time profile (in *red*) and 30-day moving average data (in *black*), (b) WPS, (c) GWS and (d) LSP for daily SSN (full solar disk) during 2010–2015.

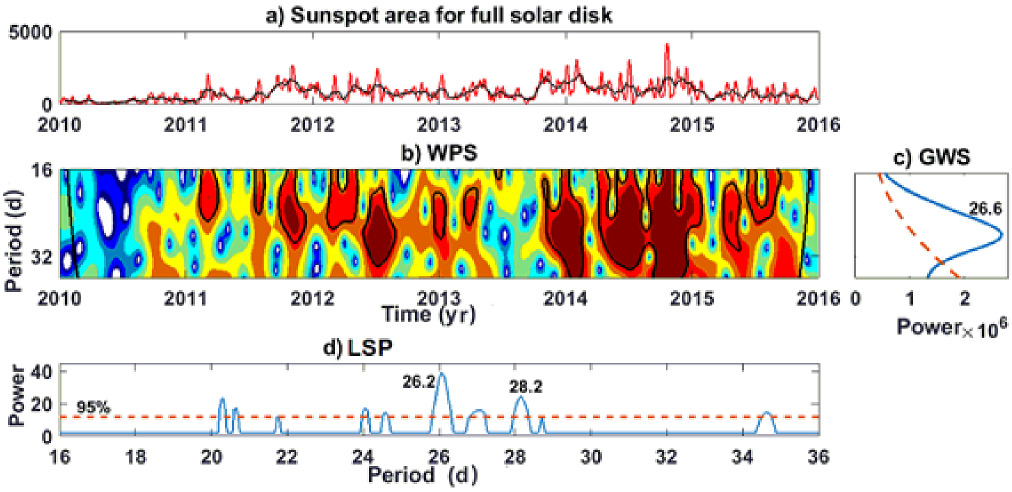


**Fig. 6** (a) Daily time profile (in *red*) and 30-day moving average data (in *black*), (b) WPS, (c) GWS and (d) LSP for daily SSA (full solar disk) during 2010–2015.

**Table 1** The percentage of months with 95% significance N-S asymmetry with respect to the total number of months for maximum phase of solar cycle 24 (2010–2015) given for SSN by paired Student's t-test. The significant months are subdivided into the northern (N) and southern (S) hemispheres.

| Year | Total Months (%) | Months-N (%) | Months-S (%) |
|---|---|---|---|
| 2010 | 50 | 50 | Nil |
| 2011 | 91.67 | 91.67 | Nil |
| 2012 | 50 | 33.33 | 16.67 |
| 2013 | 66.67 | 16.67 | 50 |
| 2014 | 91.67 | Nil | 91.67 |
| 2015 | 50 | 33.33 | 16.67 |

**Table 2** The percentage of months with 95% significance N-S asymmetry with respect to the total number of months for maximum phase of solar cycle 24 (2010-2015) given for SSA by paired Student's t-test. The significant months are subdivided into the northern (N) and southern (S) hemispheres.

| Year | Total Months (%) | Months-N (%) | Months-S (%) |
|---|---|---|---|
| 2010 | 66.67 | 58.33 | 8.33 |
| 2011 | 75 | 75 | Nil |
| 2012 | 91.67 | 50 | 41.67 |
| 2013 | 66.67 | 16.67 | 50 |
| 2014 | 75 | Nil | 75 |
| 2015 | 75 | 41.67 | 33.33 |

period variation during the time under investigation. As can be seen, for the northern hemisphere the power is mostly centered at ∼28.2 d, whereas for the southern hemisphere it is mostly centered at ∼27 d. Xiang et al. (2020), reported that the dominant rotational period of 27.4 d is present in each interplanetary magnetic field: Bx, By, and Bz when considering the daily based data in the period 1967 January 1 to 2018 December 31. Chowdhury

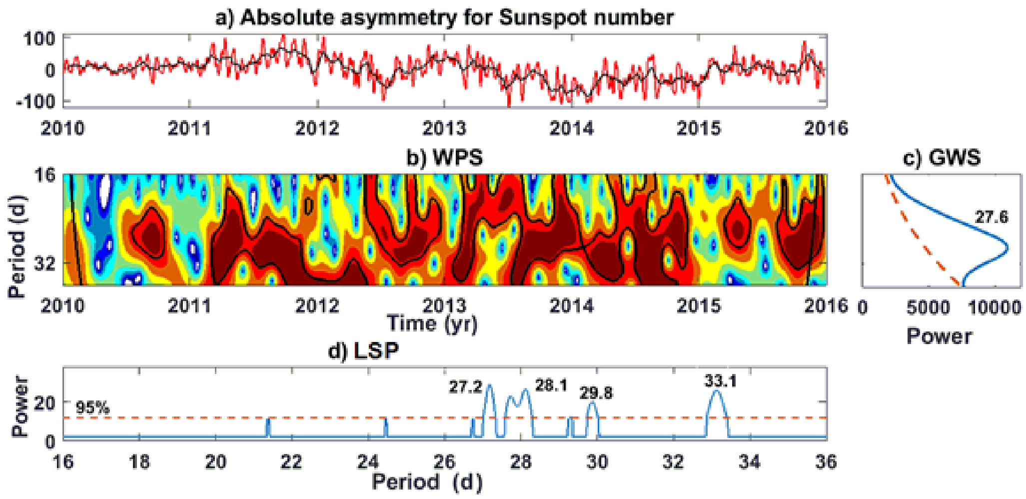


**Fig. 7** (a) Daily time profile (in *red*) and 30-day moving average data (in *black*), (b) WPS, (c) GWS and (d) LSP for daily absolute asymmetry of SSN during 2010–2015.

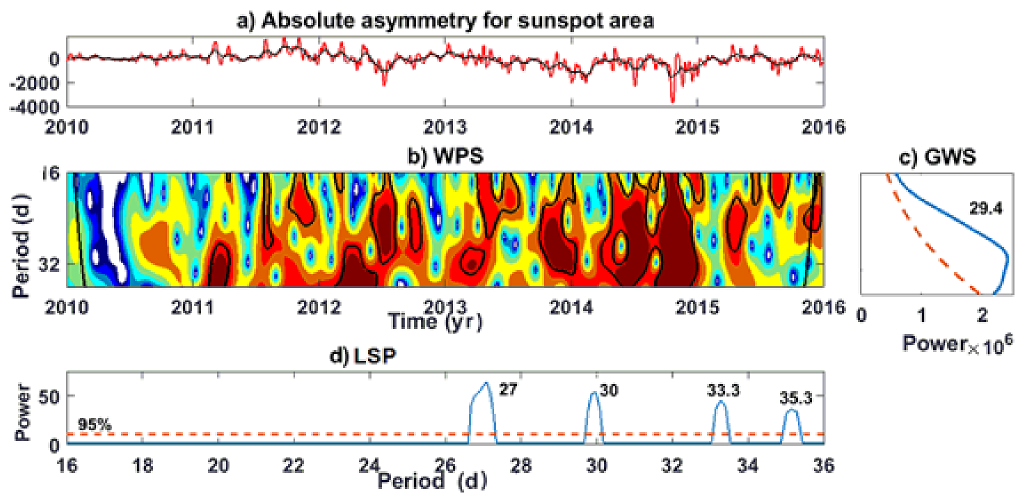


**Fig. 8** (a) Daily time profile (in *red*) and 30-day moving average data (in *black*), (b) WPS, (c) GWS and (d) LSP for daily absolute asymmetry of SSA during 2010–2015.

et al. (2015) observed quasi-periodic variations in high frequency range 10 d to 100 d during the ascending phase of the solar cycle 24. They reported that the synodic solar rotation is present in SSN/SSA, solar radio flux (F10.7), geomagnetic activity index Ap, interplanetary magnetic field (Bz) and average photospheric magnetic flux. They is also indicated that the significant period in the range of 20–31 d which mainly represents solar rotational periodicity. Singh & Badruddin (2019) observed subharmonics of fundamental period (solar rotation period 27 d) in interplanetary electric field (Ey), south ward component of magnetic field (Bz) and geomagnetic index (AE). They also reported that the subharmonics may appear simultaneously.

Consequently, these rotational periods are evidence of a strong asymmetry on both sides of the solar equator. It is the highest power that appears around the rotational period of the Sun, and it is clear around the maximum phase of solar cycle 24. This rotational property manifests a strong asymmetry with respect to the solar equator, whereas the peak is very strong. The study reveals that periodic variations of the northern and southern hemispheres of the Sun exhibit a kind of asymmetrical behavior.

Furthermore, these figures demonstrate that solar cycle 24 shows pronounced double peaks connected with solar activity maximum in the photosphere. It is evidence for the generation of a non-symmetric magnetic field in solar hemispheres. The first maximum exists due to the activity peak in the northern hemisphere, and the second is in the southern hemisphere. The second maximum was observed to be higher than the first and occurred after a change in sign of the polar magnetic field and the mean time interval

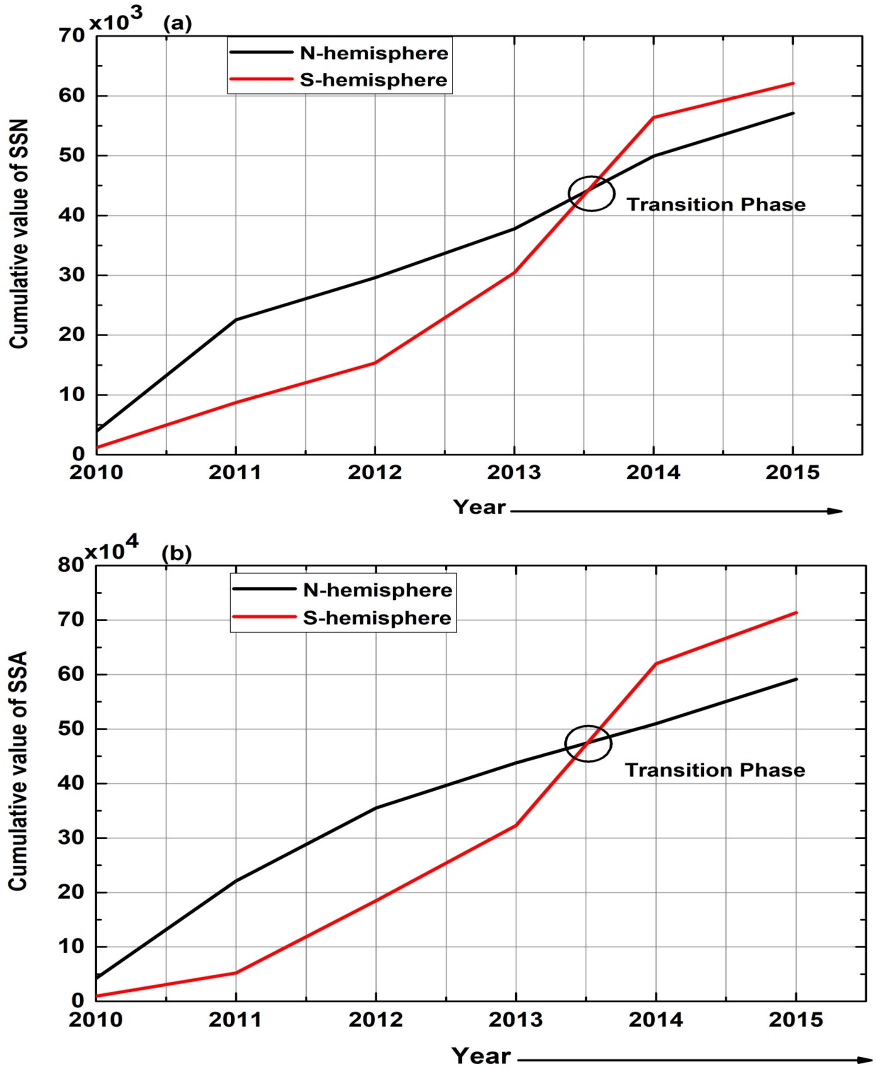


**Fig. 9** Cumulative profile for 95% significanace monthly data by using paired Student's t-test, (a) SSN and (b) SSA during 2010–2015.

between these two peaks is about 2.5 yr. This interval between two-peak structures, called the Gnevyshev gap, provides physical information about solar activity and is a superposition of northern and southern hemispheres (Gnevyshev 1967).

Figures 7(a) and 8(a) show variation of the northern hemisphere is dominant up to December 2012, but the southern hemisphere over 2013–2015. Swinson et al. (1986b) observed the N-S asymmetry of SSA and SSN, and they reported that the northern hemisphere activity peaks about two years after the sunspot minimum. Dominance of the northern hemisphere activity at the beginning of the cycle and southern hemisphere dominance after the maximum phase of the cycle has been seen and reported earlier (Singh et al. 2019b). This asymmetry flips its direction every solar cycle, which directly reveals a connection to the Hale (22-year) solar magnetic cycle (Zieger & Mursula 1998; Mursula & Zieger 2001).

From Figure 9(a) and 9(b), the circular part signifies the change of phase from the northern to southern hemisphere in terms of SSN and SSA, in turn representing an excess of magnetic flux in the later part of the solar cycle. The magnetic activity of the Sun is generally known to originate from the magnetic dynamo at the base of the solar convective zone (Pulkkinen et al. 1999). Solar magnetic activity manifests itself differently in each hemisphere and is controlled by differential rotation and meridional circulation in each hemisphere. The temporal asymmetry of meridional flow will also play a key role in the hemispheric asymmetry (Chowdhury et al. 2013).

From Tables 1 and 2, we have found above $\sim 66\%$ and $\sim 50\%$ of the monthly N-S asymmetry value with a 95% significance level for SSA and SSN respectively during the period 2010–2015. According to this result, solar activity during the period 2010–2015 is non-symmetric for the northern and southern hemispheres. The existence of N-S asymmetry has been established in solar activity phenomena. Our results support the study of Li et al. (2009) and Chowdhury et al. (2013), where the southern hemisphere dominance was observed after the transition phase.

The northern hemisphere displays an increased level of solar activity (SSNs and SSAs) during Jan 2010 to May 2013. From May 2013 to May 2015, the asymmetry becomes negative, i.e., southern hemisphere increases in the maximum phase of solar cycle 24. It is very clear that the northern and southern hemispheres individually do not exhibit the same behavior as described in the N-S asymmetry. The N-S asymmetry occurs in the maximum phase of solar cycle 24, before the reversal of the magnetic field. Vernova et al. (2002) reported that the change of dominant activity in the northern maximum to southern maximum is connected with each other.

In our results, the asymmetrical distribution of the solar activity phenomenon represents an important clue regarding the solar dynamic action. Generally, the solar activity proceeds independently in each hemisphere and is governed by the laws of differential rotation as well as meridional flows in both hemispheres (Balogh et al. 2015). Gigolashvili et al. (2003) proposed that each hemisphere has its own rotational rate which is related to the N-S asymmetry of solar activity. Georgieva & Kirov (2003) also indicated that the variations in rotational traces have different periodicities for each hemisphere. Hazra & Nandy (1974) made an attempt to explain the hemispheric asymmetry as a nonlinear coupling between the dipolar and quadrupolar components of the solar magnetic fields and indicated that parity of the Sun and hemispheric asymmetry are closely related.

The analysis of the rotational behavior for each hemisphere is of particular interest, since it is closely linked to the evolution of magnetic fields and solar dynamo. In this sense, the rotational period of the photospheric magnetic field is investigated during solar cycle 21, where it was ascertained that each hemisphere has different periods; hence a weakly coupled magnetic field is suggested between the two hemispheres. Moreover, the rotational behavior and magnetic fields originating in the two hemispheres provide strong evidence for the existence of non-symmetric solar activity (Antonucci et al. 1990). Temmer et al. (2002) revealed the same results when concerning the study of solar flares and SSNs, concluding there is a strong correlation of the rotation of the sunspots with the large-scale magnetic fields. In this regard, it should be emphasized that the N-S asymmetry largely affects many manifestations of solar activity such as the different rotational behavior of activity proxies in each hemisphere and the preference of one hemisphere over the other.

The reversal of the polar magnetic field during solar cycle 24 has been investigated by many studies which give inconsistent results. For instance, Gopalswamy et al. (2016) reported that the reversal in the southern hemisphere took place during June 2014 and in the northern hemisphere around October 2012. However, multiple reversals observed in the northern hemisphere were completed by Jun 2012, and only a single reversal in the southern hemisphere was found from Jan 2013 to November 2014 (Janardhan et al. 2018). Such unusual delayed and prolonged reversal by more than 2 years is attributed to faster meridional flow speed in the north than the south. Also, Svalgaard & Kamide (2013) suggested that the occurrence of multiple peaks associated with different polar reversal times is considered as an intrinsic property of the solar cycle. Moreover, they attributed the asynchronous reversal of the Sun's polar field as a consequence of the N-S asymmetry of solar activity.

To conclude, the study affirms that periodic variations in the solar rotational period ($\sim$27 d) in the northern and southern hemispheres of the Sun demonstrate a kind of asymmetrical behavior. The value of synodic solar rotation is very consistent with the result in Xiang et al. (2020) and references therein. The rotational nature of the northern and southern hemispheres is relevant, and it is interconnected with the solar dynamo and magnetic field generation. The peak value (maximum) of the northern and southern hemisphere is not reached simultaneously. It is a shift of several months (approximately 30 months). The peak of SSN and SSA (a combination of the northern and southern hemispheres) yields a shift of several months and is the well-known Gnevyshev gap. Besides, the study of solar activity asymmetry imposes limitations on the theories of a solar dynamo being able to explain the presence of severe N-S asymmetry in the observation of solar activity as well as in the rotational behavior and the weak coupling between the two hemispheres.

## References

Antonucci, E., Hoeksema, J. T., & Scherrer, P. H. 1990, ApJ, 360, 296

Ataç, T., & Özgüç, A. 1996, Sol. Phys., 166, 201

Balogh, A., Hudson, H., Petrovay, K., & Steiger, R. Eds. 2015, Introduction to the Solar Activity Cycle: Overview of Causes and Consequences, 53, https://doi.org/10.1007/978-1-4939-2584-1_1

Balthasar, H., & Schüssler, M. 1984, Sol. Phys., 93, 177

Ballester, J. L., Oliver, R., & Carbonell, M. 2005, A&A, 431, L5

Bartels, J. 1934, Terrestrial Magnetism and Atmospheric Electricity (Journal of Geophysical Research), 39, 201
Carbonell, M., Oliver, R., & Ballester, J. L. 1993, A&A, 274, 497
Charbonneau, P. 2020, Living Reviews in Solar Physics, 17, 4
Chowdhury, P., Choudhary, D. P., & Gosain, S. 2013, ApJ, 768, 188
Chowdhury, P., Choudhary, D. P., Gosain, S., et al. 2015, Ap&SS, 356, 7
Chowdhury, P., & Kudela, K. 2018, Ap&SS, 363, 250
Chowdhury, P., Kilcik, A., Yurchyshyn, V., et al, J. P. 2019, Sol. Phys., 294, 142
El-Borie, M. A., El-Taher, A. M., Thabet, A. A., et al. 2019, ApJ, 880, 86
Georgieva, K., & Kirov, B. 2003, ESA Special Publication, 517, 275
Gigolashvili, M. S., Japaridze, D. R., Mdzinarishvili, T. G., et al. 2005, Sol. Phys., 227, 27
Gigolashvili, M. S., Mdzinarishvili, T. G., Japaridze, D. R., et al. 2003, New Astron., 8, 529
Gnevyshev, M. N. 1967, Sol. Phys., 1, 107
Gopalswamy, N., Yashiro, S., & Akiyama, S. 2016, ApJL, 823, L15
Hathaway, D. H. 2015, Living Reviews in Solar Physics, 12, 4
Hazra, S., & Nandy, D. 2019, MNRAS, 489, 4329
Howard, R. 1974, Sol. Phys., 38, 59
Janardhan, P., Fujiki, K., Ingale, M., et al. 2018, A&A, 618, A148
Javaraiah, J. 2016, Ap&SS, 361, 208
Javaraiah, J. 2019, Sol. Phys., 294, 64
Kilcik, A., Yurchyshyn, V., et al. 2018, Sol. Phys., 293, 63
Knaack, R., Stenflo, J. O., & Berdyugina, S. V. 2004, A&A, 418, L17
Leussu, R., Usoskin, I. G., Senthamizh Pavai, V., et al. 2017, A&A, 599, A131
Li, K. J., Chen, H. D., Zhan, L. S., et al. 2009, Journal of Geophysical Research (Space Physics), 114, A04101
Li, K. J., Liu, X. H., Gao, P. X., & Zhan, L. S. 2010, New Astron., 15, 346
Li, K. J., Wang, J. X., Xiong, S. Y., et al. 2002, A&A, 383, 648
Lomb, N. R. 1976, Ap&SS, 39, 447
Mursula, K., & Zieger, B. 2001, Geophys. Res. Lett., 28, 95
Oliver, R., & Ballester, J. L. 1994, Sol. Phys., 152, 481
Poblet, F. L., & Azpilicueta, F. 2018, Advances in Space Research, 61, 2275
Pulkkinen, P. J., Brooke, J., Pelt, J., & Tuominen, I. 1999, A&A, 341, L43
Rusin, V. 1980, Bulletin of the Astronomical Institutes of Czechoslovakia, 31, 9
Scargle, J. D. 1982, ApJ, 263, 835
Singh, P. R., Tiwari, C. M., Agrawal, S. L., & Pant, T. K. 2019a, Sol. Phys., 294, 118
Singh, P. R., Tiwari, C. M., Saxena, A. K., Agrawal, S. L., & Mishra, A. P. 2019b, Ap&SS, 364, 59
Singh, Y. P., & Badruddin, 2019, Astrophysics and Space Science, 364, 200
Svalgaard, L., & Kamide, Y. 2013, ApJ, 763, 23
Swinson, D. B., Koyama, H., & Saito, T. 1986a, Sol. Phys., 106, 35
Swinson, D. B., Shea, M. A., & Humble, J. E. 1986b, J. Geophys. Res., 91, 2943
Temmer, M., Rybák, J., Bendík, P., et al. 2006, A&A, 447, 735
Temmer, M., Veronig, A., & Hanslmeier, A. 2002, A&A, 390, 707
Torrence, C., & Compo, G. P. 1998, Bulletin of the American Meteorological Society, 79, 61
Vernova, E. S., Mursula, K., Tyasto, M. I., & Baranov, D. G. 2002, Sol. Phys., 205, 371
Vizoso, G., & Ballester, J. L. 1990, A&A, 229, 540
Waldmeier, M. 1971, Sol. Phys., 20, 332
White, O. R., & Trotter, D. E. 1977, ApJS, 33, 391
Xiang, N. B., Ning, Z. J., & Li, F. Y., 2020, ApJ, 896, 12
Zieger, B., Mursula, K. 1998, Geophys. Res. Lett., 25, 841